

Superplastic behaviour of friction stir processed AZ91 magnesium alloy produced by high pressure die cast

P. Cavaliere*, P.P. De Marco

INFM-Department of "Ingegneria dell'Innovazione", Engineering Faculty, University of Lecce, Via per Arnesano, 73100 Lecce, Italy

Received 15 June 2006; received in revised form 9 October 2006; accepted 8 November 2006

Abstract

The room temperature and hot tensile properties of AZ91 magnesium alloy produced by high pressure die cast after friction stir processing (FSP) were studied in the present paper. Such process is a modification of classical friction stir welding one in which the sheets are not joined but the stirring action of the tool, on the bulk material, is used to refine the microstructure in order to increase the mechanical properties of the metal such as yield strength, fatigue life and possible superplastic properties at relative low temperature and high strain rates [R.S. Mishra, Z.Y. Ma, Mater. Sci. Eng. R 50 (2005) 1–78]. The material was FSP after solution treatment and the superplastic behaviour was analysed by means of hot tensile tests, in longitudinal direction, in the temperature and strain rate ranges of 225–300 °C and 10^{-2} to 10^{-4} s⁻¹, respectively.

© 2006 Elsevier B.V. All rights reserved.

Keywords: FSP; AZ91; Superplasticity

1. Introduction

Magnesium alloys components are very attractive for industrial applications in the transportation field because of their low density and the excellent room temperature strength and rigidity [2–4]. However, the use of magnesium alloys has been strongly limited because of their poor formability at near room temperature as a consequence of hcp lattice. Many results have been published on the physical and mechanical properties of AZ91 and other magnesium alloys in particular, demonstrating the existence of superplastic behaviour [5–8]. It is clear that it is possible to achieve superplasticity at high strain rates, in conventional alloys, by making a strong reduction in grain size; this can be obtained by using a process such as Equi-Channel-Angular pressing, high pressure torsion or friction stir processing in which the samples are subjected to a severe plastic deformation leading to a strong grain refinement [9,10].

In the friction stir processing, a rotating tool, with a specially designed rotating probe, travels down the surfaces of metal plates, and produces a highly plastically deformed zone through the associated stirring action. The localized thermo-mechanical

affected zone is produced by friction between the tool shoulder and the plate top surface, as well as plastic deformation of the material in contact with the tool [11]. The probe is typically slightly shorter than the thickness of the work piece and its diameter is typically the thickness of the work piece [12]. The friction stir processing (FSP) process is a solid-state process and therefore solidification structure is absent and the problem related to the presence of brittle inter-dendritic and eutectic phases is eliminated [13].

The frictioned zone consists of a weld nugget, thermo-mechanically affected zone (TMAZ) and a heat affected zone (HAZ). The process results in the obtaining of a very fine and equiaxed grain structure in the weld nugget obtained through a continuous dynamical recrystallization process causing a higher mechanical strength and ductility, the strong grain refinement produced by the process lead the microstructure to the fine dimensions proper of the possibility to exhibit superplastic properties [14–16].

The aim of the present study is the investigation of the effect of the FSP on the microstructure modifications of AZ91 magnesium alloy and the subsequent effect on the superplastic forming behaviour of HPDC sheets. Previous studies from the authors, in fact, demonstrated a strong increase in such properties for the AM60B magnesium alloy commonly known as difficult formable materials [17].

* Corresponding author. Tel.: +39 083 2297324; fax: +39 083 2325004.
E-mail address: pasquale.cavaliere@unile.it (P. Cavaliere).

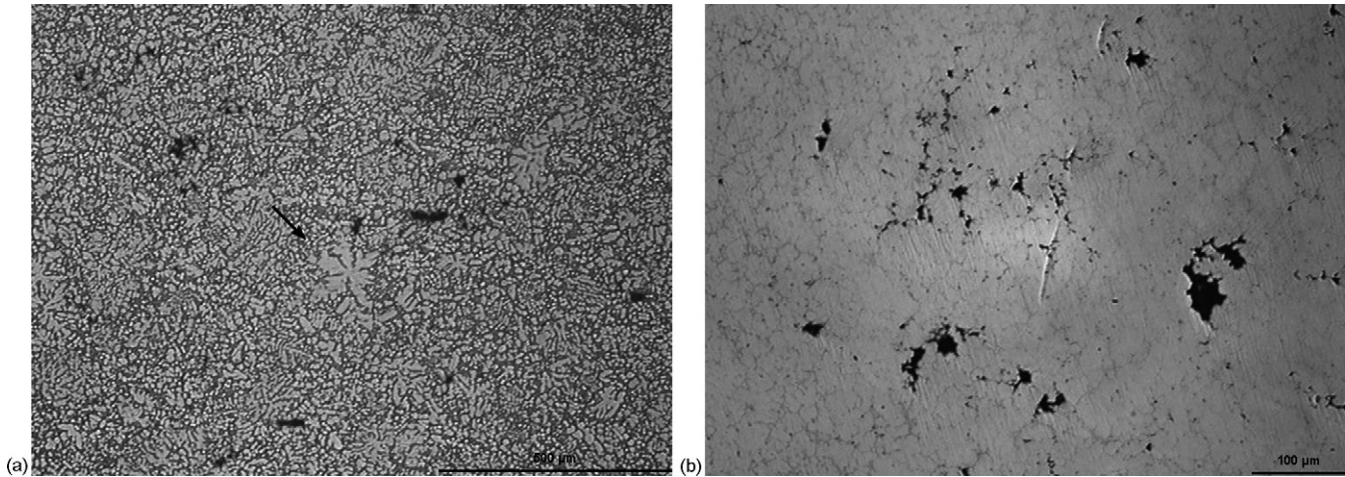


Fig. 1. Microstructure of the as-cast material after etching (a) and in non-etched (b) condition showing isolated zones of voids.

2. Experimental procedure

The material under investigation was an AZ91 magnesium alloy with the following composition (wt%): Al, 8.9; Zn, 0.79; Si, 0.0093; Cu, 0.0013; Ni, 0.001; Fe, 0.0017; Be, 36 ppm; Mg, bal. The material was produced by HPDC into the form of special trials of 2.5 mm thickness. The material was solution treated at 415 °C for 2 h in order to soften the alloy before tool processing. In this way, in fact, it is possible to reduce the tool rotation speed with a reduction of materials heating and subsequent stronger grain refinement during the stirring. Then, the material was subjected to friction stir processing by employing a flat C60 steel tool with rotating speed of 700 rpm and a travelling speed of 2.5 mm/s, the tool was rotated in the clockwise direction while the specimens, fixed at the backing plate, were moved. The nib was 2.5 mm in diameter and 2.4 mm long, and a 20 mm diameter shoulder was machined perpendicular to the axis of the tool; the tilt angle of the tool was 3° [18].

The Vickers hardness profile of the material was measured on a cross-section and perpendicular to the processing direction using a Vickers indenter with a 200 gf load for 15 s.

To determine the tensile strength of the stirred zone, tensile test specimens were sectioned in the longitudinal direction along the processing line with an electrical discharge machine (EDM). The tensile test was carried out at room temperature using an MTS 810 testing machine with initial strain rate of 10^{-3} s^{-1} .

Hot tensile tests were performed in order to evaluate the superplastic properties of the material obtained by FSP process in the temperature and strain rate ranges 225–300 °C and 10^{-2} to 10^{-4} s^{-1} , respectively, by employing specimens obtained by EDM from the nugget zone cut parallel to the processing direction; before tests, the surfaces of the specimens were mechanically polished in order to eliminate all the possible surface defects effects. The tensile tests were carried out using a LLOYD Instruments LR5K testing machine equipped with a resistance furnace.

The strain rate sensitivity coefficient (m) of the material was calculated employing the following equation:

$$m = \left. \frac{\partial \log \sigma}{\partial \log \dot{\epsilon}} \right|_{\epsilon, T} \quad (1)$$

The m value was calculated by interpolating the data obtained by hot tensile curves at an equivalent strain of 1. The cubic interpolation was applied between σ and $\dot{\epsilon}$ logarithmic values.

Surfaces were prepared by standard metallographic techniques and etched with acetic–picral (10 ml acetic acid, 4.2 g picric acid, 10 ml water and 70 ml ethanol) and acetic–glycol (1 ml nitric acid, 20 ml acetic acid, 60 ml glycoletilene con 19 ml water) etchings for microstructural observations.

3. Results and discussion

The as-received material was characterized by the classical cast structure in which different floating crystals can be recognized (Fig. 1a). In the same specimens randomly distributed zones characterized by large porosity have been observed (Fig. 1b). Both the etchings used in the present study revealed the formation of primary α grains (light) embedded in the dark eutectic β phase ($\text{Mg}_{17}\text{Al}_{12}$); the material etched in both ways is shown in Fig. 2. The divorced eutectic phase of the as-received material was put in evidence by the observations performed by employing the FEGSEM microscope (Fig. 3a and b).

The microstructure of the material after solution treatment is shown in Fig. 4, there are visible the recrystallized grains with eutectic β ($\text{Mg}_{17}\text{Al}_{12}$) phase at the grain boundaries.

After FSP, no macroscopic defects were observed in the stirred sheets. In addition, no voids were observed in different observed sections, this is consistent with the results obtained by previous studies [19,20], too high rotation speeds can produce,

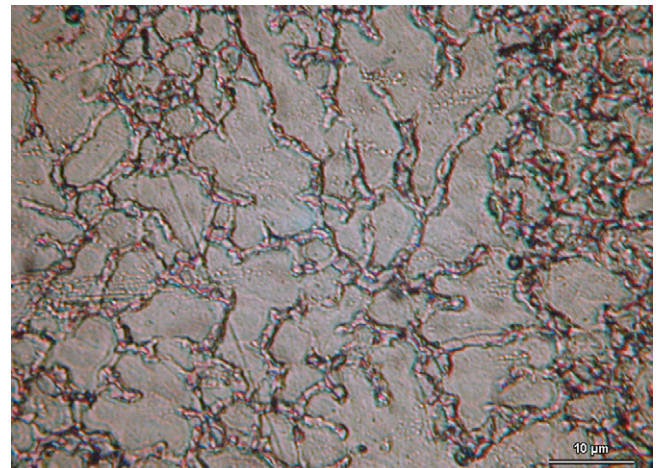


Fig. 2. Primary α grains (light) embedded in the dark eutectic β phase ($\text{Mg}_{17}\text{Al}_{12}$).

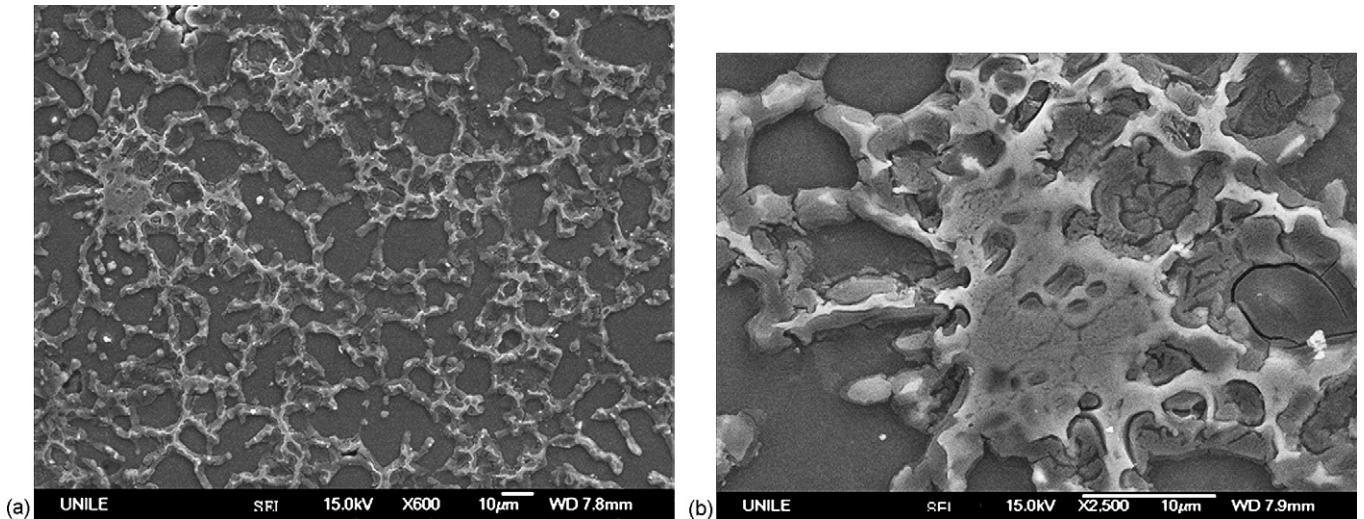


Fig. 3. (a and b) Divorced eutectic phase of the as-received material put in evidence by the observations performed by employing the FEGSEM microscope.

in fact, cracks, cavities and generation of liquid phases in the material.

Light microscopy observations were widely performed on the transverse cross-sections of the FSP specimens, the stirred AZ91 HPDC magnesium alloy revealed the classical formation of the elliptical “onion” structure in the centre of the specimen; this is a structure characterized by fine and equiaxed recrystallized grains (Fig. 5), the higher temperature and severe plastic deformation results in grains recrystallized with a strong different structure respect to the as-cast as-received material, no porosity was observed in the stirred zone; a statistical analysis on 200 grains lead to a measurement of a mean grain size of 4 µm.

At a distance of 4 mm from the centre many of the prior grains and eutectic phase of the parent material start to appear (Fig. 6). This region corresponds to the heat affected zone as the hardness is low compared to the base metal. The hardness drops here because the precipitates are coarsened. In the region adjacent to the nugget, i.e. TMAZ no recrystallization is observed

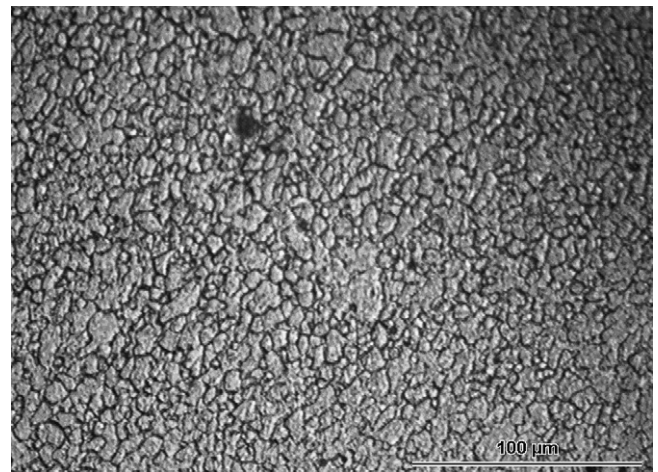


Fig. 5. Structure characterized by fine and equiaxed recrystallized grains in the nugget zone of the FSP material.

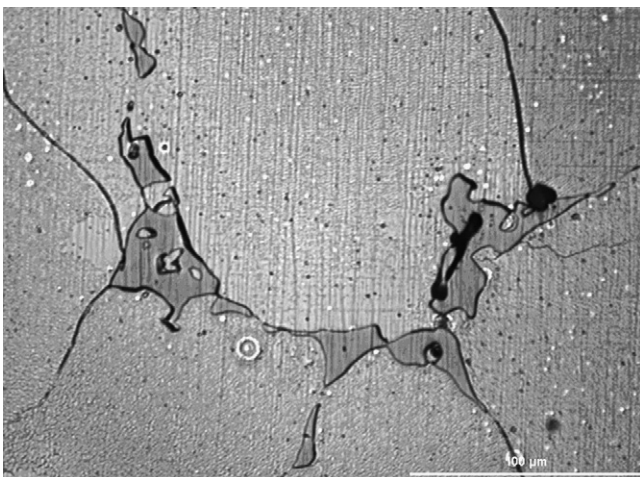


Fig. 4. Recrystallized grains with eutectic β ($Mg_{17}Al_{12}$) phase at the grain boundaries in the solution treated condition.

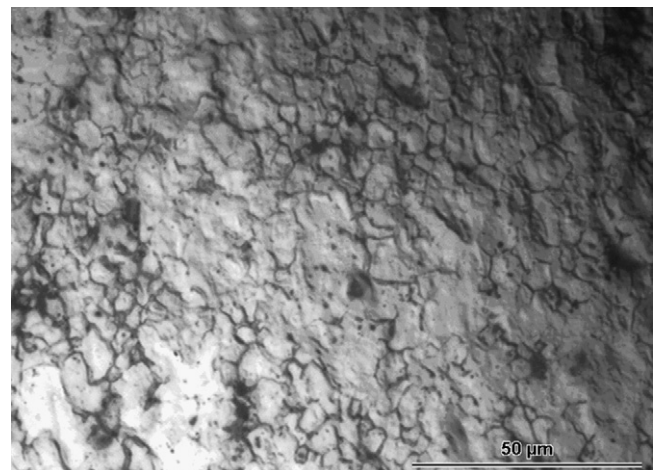


Fig. 6. Prior grains and eutectic phase of the parent material observed in the TMAZ.



Fig. 7. Structure observed in the HAZ of the FSP material.

because the temperature derived from the friction stir processing is not high enough and the deformation is not so severe to cause recrystallization (Fig. 7).

Such behaviour is confirmed by the microhardness profile (Fig. 8) along the FSP roads, the microhardness reaches a value of 91 Hv in the centre of the stirred zone and then it starts to decrease after 2.5 mm from the centre until reaching a plateau corresponding to the hardness values of the parent material. The hardness of the joint reaches lower values in the HAZ and TMAZ with respect to nugget, in the HAZ and TMAZ, in fact, the competing mechanisms of work hardening and over-ageing produce a strength decreasing respect to the stirred zone.

FSP is becoming a very important solid-state technique to obtain superplastic sheets especially from the material belonging to the nugget zone. In this zone, in fact, the grains are subjected to a forging/extrusion process with a true strain of about 13–15 (at very high strain rates) which produce a strong dynamic recrystallization and a several grain rotation which leads to a structure characterized by fine high misoriented grain

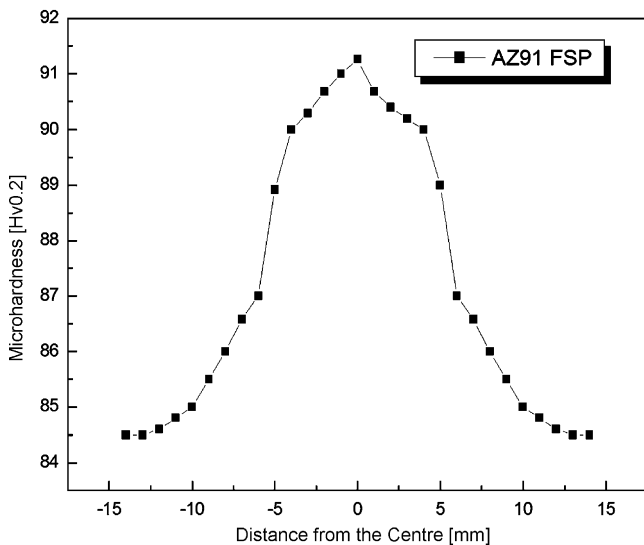


Fig. 8. Microhardness profile in the cross-section of the FSP roads.

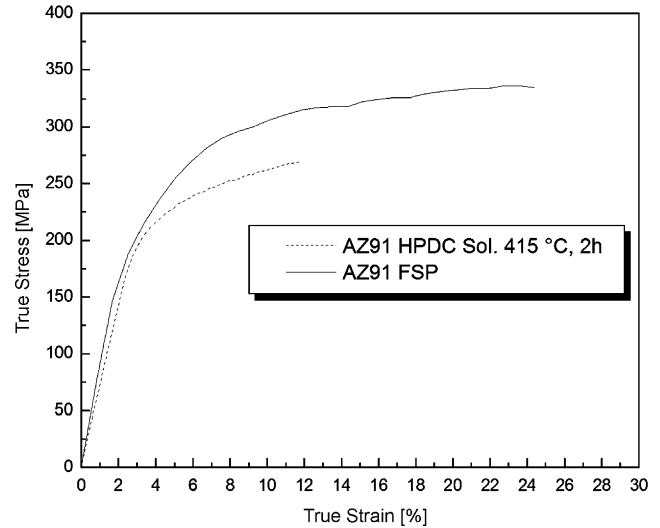


Fig. 9. Tensile behaviour of the studied material in the as solutioned and FS processed conditions.

boundaries which is the fundamental condition for superplastic properties [1].

The tensile behaviour of the studied material in the as solution treated and FS processed conditions is plotted in Fig. 9. The FSP produces a strong increase in mechanical properties respect to the unstirred material with an increase in the elongation to failure accompanied with a strong increase in strength due to the very fine recrystallized structure and to the absence of porosity produced by the stirring process. In the HPDC as-received material, in fact, large porosities and oxides formation were observed on the fracture surfaces (Fig. 10). Such voids disappear after FSP and no oxides presence was observed on the fracture surfaces (Fig. 11). The oxides particles are, in fact, broken in a very fine shape from the tool action and reduced to a very smaller dimension respect to than in the case of as-cast material [20–22].

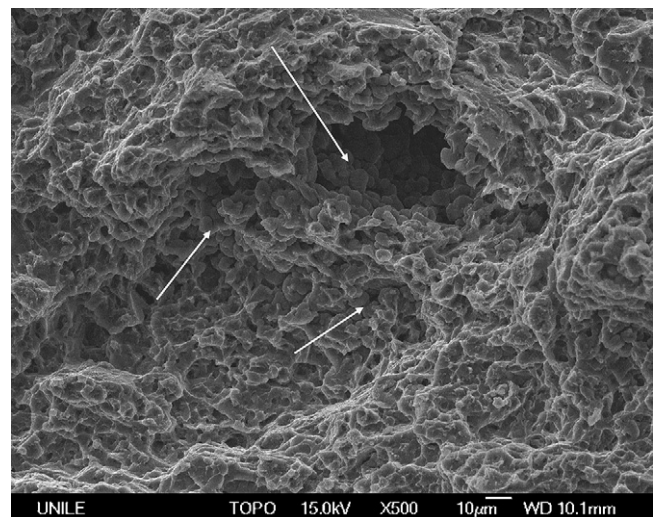


Fig. 10. Fracture surfaces of the as-received tensile tested material showing voids and oxides formation.

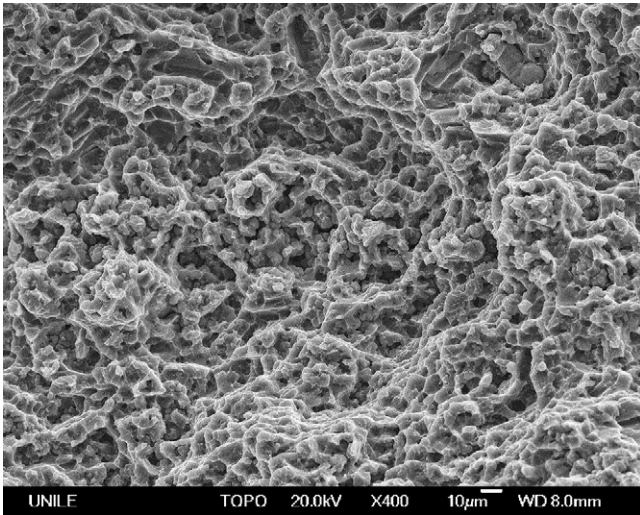


Fig. 11. Fracture surfaces of the FSP tensile tested material.

The true stress versus true strain curves obtained in different conditions of strain rates and temperature showed a net increase in stress with strain up to a peak, at the lower strain rate investigated the peak was followed by a strong flow softening in all the temperatures conditions. Fig. 12 summarizes the flow stress behaviour of the material as a function of strain rate at all the testing temperatures of the present study in a form of double logarithmic plot, the value used in the plot is relative to a true strain of 0.2.

A superplastic typical sigmoidal behaviour of the flow stress with the initial strain rate for all the investigated temperatures identifying three different regions of superplastic deformation was recognized, an increase in flow stress as increasing strain rate and decreasing temperature was observed for all the studied conditions. The material is subjected, during the stirring action, to a severe plastic deformation which produces recrystallization and development of texture, such grains are characterized by

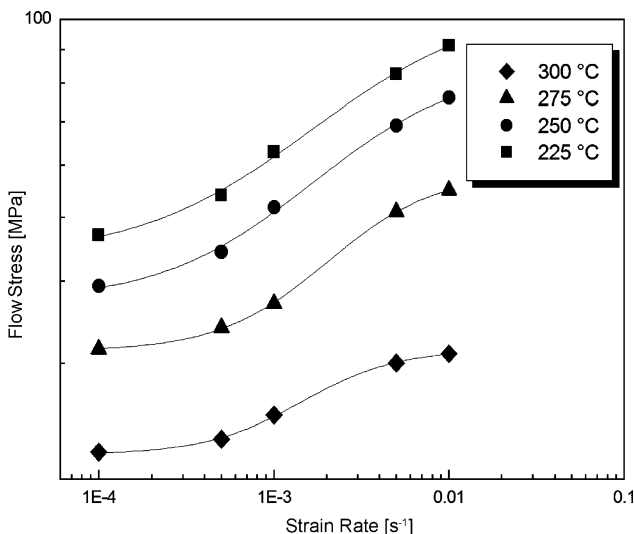


Fig. 12. Flow stress behaviour of the material as a function of strain rate at all the testing temperatures.

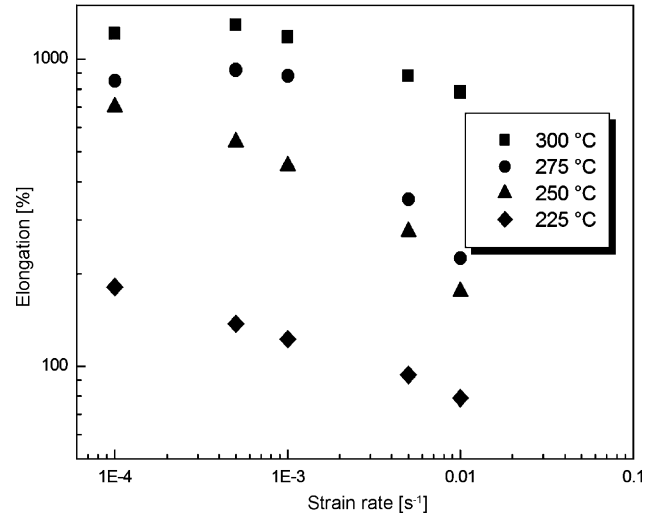


Fig. 13. Variation of the total elongation to failure as a function of the different initial strain rate.

high angles and low dislocation density as reported in previous studies [23–25]. Such process, normally known as continuous dynamic recrystallization, is characterized by subgrain rotation and high misorientation without grain migration [26]. In particular, the low angle boundaries of the parent material are replaced by high angle boundaries through a continuous rotation for the tool action.

The variation of the total elongation to failure as a function of the different initial strain rate is shown in Fig. 13, the tensile ductility increase as increasing the strain rate for the higher temperatures investigated (275–300 °C) in the intermediate strain rates investigated, the fine and stable grain structure leads to the exhibition of exceptional ductility respect to the unmodified alloy in friction stir processed conditions.

As it can be seen in Fig. 14, the maximum of the strain rate sensitivity ($m = 0.68$), calculated at a true strain of 0.2, is high at temperature ranging from 275 to 300 °C.

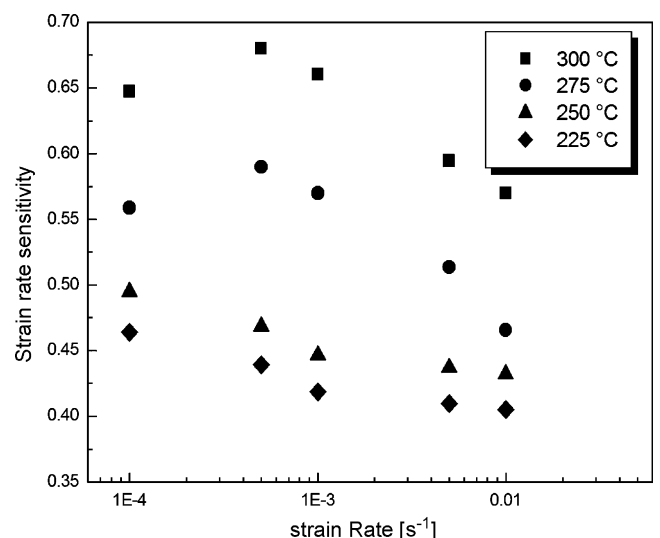


Fig. 14. Variation of strain rate sensitivity as a function of the different initial strain rate.

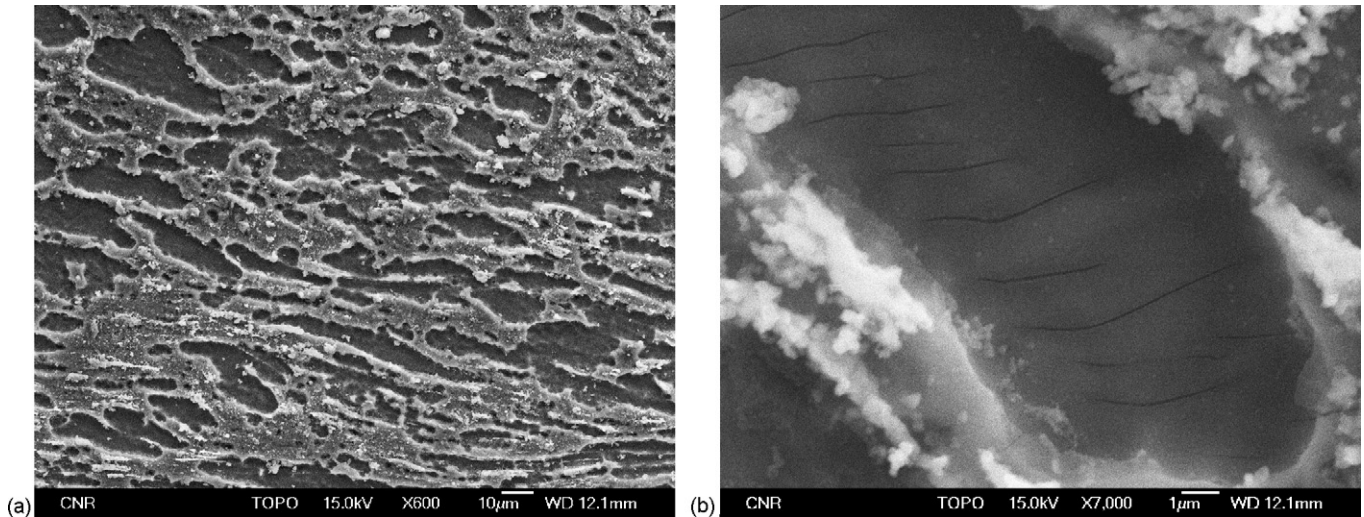


Fig. 15. Transversal observations of tensile tested specimens ($300\text{ }^{\circ}\text{C}$, $5 \times 10^{-4}\text{ s}^{-1}$) revealing grain boundary sliding (a) and twinning deformation (b).

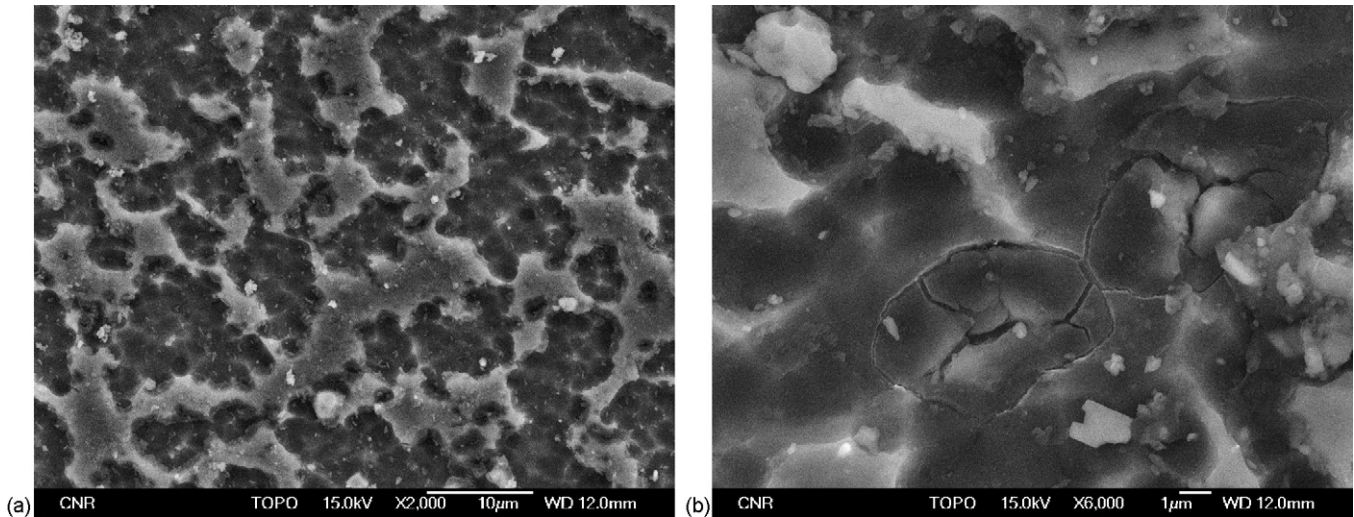


Fig. 16. Transversal observations of tensile tested specimens ($250\text{ }^{\circ}\text{C}$, $5 \times 10^{-4}\text{ s}^{-1}$) revealing no-grain boundary sliding (a) and triple-junctions fracture (b).

The low temperatures, the maximum of the strain rate sensitivity is relatively lower than that in the high one. It was observed a characteristic feature of the superplastic behaviour of the material with a high strain rate sensitivity of the flow stress. In addition, very large elongations were observed in the temperature and strain rate ranges, where high m values were found ($>1000\%$); the maximum ductility (1050%) and the highest m values (0.68) were recorded in the intermediate superplastic region. Such behaviour was confirmed by the SEM observations performed on the transversal sections of tensile tested specimens, for the intermediate flow stresses and higher temperatures investigated ($275\text{--}300\text{ }^{\circ}\text{C}$) a strong deformation related to grain boundary sliding was observed (Fig. 15) inside the grains a typical twinning deformation behaviour was revealed. On the contrary, at the same strain rates and lower temperatures no grain boundary sliding was observed and the material was characterized by triple-junctions fracture (Fig. 16).

4. Conclusions

The effect of friction stir processing on the superplastic behaviour of a AZ91 magnesium alloy was investigated in the present study. The material was friction stir processed showing good strength and ductility values at room temperature because of the very fine structure obtained by the processing, revealing an increase in room temperature ductility respect to the unstirred material. The tensile tests performed in the temperature range $275\text{--}300\text{ }^{\circ}\text{C}$ at different strain rates showed the occurrence of high ductility and high strain rate sensitivity levels.

References

- [1] R.S. Mishra, Z.Y. Ma, Mater. Sci. Eng. R 50 (2005) 1–78.
- [2] T.G. Langdon, Mater. Trans. 40 (1999) 716–722.
- [3] B.L. Mordike, T. Ebert, Mater. Sci. Eng. A 302 (2001) 37–45.

- [4] K. Máthis, Z. Trojanová, P. Lukác, C.H. Cáceres, J. Lendvai, J. Alloys Compd. 378 (2004) 176–179.
- [5] A. Rudajevova', M. Stanek, P. Lukác, Mater. Sci. Eng. A 341 (2003) 152–157.
- [6] H. Wetanabe, T. Mukai, M. Kohzu, S. Tanabe, K. Higashi, Mater. Trans. 40 (1999) 809–841.
- [7] M. Mabuki, K. Ameyama, H. Iwasaki, K. Higashi, Acta Mater. 47 (1999) 2047–2054.
- [8] A. Bussiba, A. Ben Artzy, A. Shtechman, S. Ifergan, M. Kupiec, Mater. Sci. Eng. A 302 (2001) 56–62.
- [9] I. Charit, R.S. Mishra, Mater. Sci. Eng. A 359 (2003) 290–296.
- [10] Z.Y. Ma, R.S. Mishra, M.W. Mahoney, Scripta Mater. 50 (2004) 931–935.
- [11] M. Guerra, C. Schmidt, J.C. McClure, L.E. Murr, A.C. Nunes, Mater. Charact. 49 (2003) 95–101.
- [12] P. Ulysse, Int. J. Mach. Tools Manuf. 42 (2002) 1549–1557.
- [13] C.G. Rhodes, M.W. Mahoney, W.H. Bingel, Scripta Mater. 36 (1997) 69–75.
- [14] H.G. Salem, A.P. Reynolds, J.S. Lyons, Scripta Mater. 46 (2002) 337–342.
- [15] C.G. Rhodes, M.W. Mahoney, W.H. Bingel, M. Calabrese, Scripta Mater. 48 (2003) 1451–1455.
- [16] Y.S. Sato, M. Urata, H. Kokawa, K. Ikeda, Mater. Sci. Eng. A 354 (2003) 298–305.
- [17] P. Cavaliere, P.P. De Marco, J. Mater. Sci. 41 (2006) 3459–3464.
- [18] P. Cavaliere, G. Campanile, F. Panella, A. Squillace, J. Mater. Process. Technol. 180 (2006) 263–270.
- [19] W.B. Lee, Y.M. Yeon, S.B. Jung, Mater. Sci. Technol. 19 (2003) 785.
- [20] S.H.C. Park, Y.S. Sato, H. Kokawa, in: S.A. David, T. DebRoy, J.C. Lippold, H.B. Smartt, J.M. Vitek (Eds.), Proceedings of the Sixth International Conference on Trends in Welding Research, Pine Mountain, GA, ASM International, 2003, p. 267.
- [21] K.V. Jata, K.K. Sankaran, J.J. Ruschau, Metall. Mater. Trans. A 31 (2000) 2181.
- [22] W.B. Lee, J.W. Kim, Y.M. Yeon, S.B. Jung, Mater. Trans. 44 (2003) 917.
- [23] W.B. Lee, Y.M. Yeon, S.B. Jung, Mater. Sci. Technol. 19 (2003) 785.
- [24] C.G. Rhodes, M.W. Mahoney, W.H. Bingel, M. Calabrese, D. Waldron, Scripta Mater. 36 (1997) 69.
- [25] G. Liu, L.E. Murr, C.S. Niou, J.C. McClure, F.R. Vega, Scripta Mater. 37 (1997) 355.
- [26] K.V. Jata, S.L. Semiatin, Scripta Mater. 43 (2000) 743.